Avrupa Bilim ve Teknoloji Dergisi
Sayı 35, S. 288-294, Nisan 2022

Araştırma Makalesi

www.ejosat.com ISSN:2148-2683

European Journal of Science and Technology
No. 35, pp. 288-294, April 2022

Research Article

An Efficient Brushless DC Motor Design for Unmanned Aerial Vehicles

Yusuf Yaşa[1*]

[1*] Bursa Technical University, Faculty of Faculty of Engineering and Natural Sciences, Departmant of Electrical Engineering, Bursa, Turkey, (ORCID: 0000-0002-2032-9810), yusuf.yasa@btu.edu.tr

(First received 7 March 2022 and in final form 25 March 2022)

(**DOI:** 10.31590/ejosat.1083838)

ATIF/REFERENCE: Yaşa, Y. (2022). An Efficient Brushless DC Motor Design for Unmanned Aerial Vehicles. *European Journal of Science and Technology*, (35), 288-294.

Abstract

In this study, 650W, 3500rpm 225Kv with 5kg traction force brushless DC motor is developed by using multidisciplinary analysis tools which include electrical, electromagnetics and electronics. In aerial vehicles, the efficiency is highly significant since it affects whole system parameters such as flight time, battery capacity, system mass and its acoustic noise level etc. Electric motor designer's aim is to increase machine efficiency at particular operating condition which is usually at rated condition. However, in aerial vehicles the motor's load type is fan and it has a parabolic speed-torque characteristic. Hence, the motor efficiency should be maximized in this particular load line in a wide speed range. Hence, the study mostly focuses on maximizing the electrical energy to traction force conversion efficiency at fan load characteristic but other performance-enhancing studies have not been neglected. The performance metrics will be more detailed in the study. The results are verified with both simulation and experimental study.

Keywords: Aerial vehicles, Brushless DC motor, Motor efficiency.

İnsansız Hava Araçları İçin Verimli Bir Fırçasız DC Motor Tasarımı

Öz

Bu çalışmada, elektrik, elektromanyetik ve elektroniği içeren multidisipliner analiz araçları kullanılarak 650W, 3500rpm 225Kv 5kg çekiş gücüne sahip fırçasız DC motor geliştirilmiştir. Hava araçlarında verimlilik, uçuş süresi, pil kapasitesi, sistem kütlesi ve akustik gürültü seviyesi gibi tüm sistem parametrelerini etkilediği için oldukça önemlidir. Elektrik motoru tasarımcısının amacı, genellikle nominal olan belirli çalışma koşullarında makine verimliliğini artırmaktır. Ancak hava araçlarında motorun yük tipi fandır ve parabolik hız-tork karakteristiğine sahiptir. Bu nedenle, geniş bir hız aralığında bu özel yük hattında motor verimi maksimize edilmelidir. Bu nedenle, çalışma çoğunlukla fan yük karakteristiğinde elektrik enerjisinin çekiş kuvveti dönüşüm veriminin maksimize edilmesine odaklanmaktadır, ancak diğer performans artırıcı çalışmalar ihmal edilmemiştir. Performans metrikleri çalışmada daha ayrıntılı olarak anlatılacaktır. Sonuçlar hem simülasyon hem de deneysel çalışma ile doğrulanmıştır.

Anahtar Kelimeler: İnsansız hava araçları, Fırçasız DC motor, Motor verimi.

[*] Corresponding Author: yusuf.yasa@btu.edu.tr

1. Introduction

Drones or quadracopters are playing an important role in various sectors such as logistics, transportation, toys, military, agricultural applications etc(Mithra, 2021). Today's market shows that the applications where drones will penetrate will increase even more(Taha, 2022). One of the most critical parts in the drone system is electric traction motors. They consume most of the stored energy in the operation. While the motors keep the drone in the air, it also undertakes the routing task of the drone. Hence, its operating efficiency is critical and needs to be maximized. Otherwise, drone operating time would be shortened. In a simple way, efficiency can be increased by making electric motor big, however, in this case, the drone becomes heavier and the operation time is shortened, again. Hence, maximizing efficiency by keeping the motor mass same should be one of the biggest goal in the unmanned aerial vehicles(Emanuele, 2021).

Electric motors convert electrical energy to the mechanical traction energy with rotary motion. In the unmanned aerial vehicles, electric motors work with the principle of attraction or repulsion of two magnetic fields; rotor and stator magnetic fluxes. The rotor magnetic flux source is the permanent magnet in the BLDC motors. However, the stator flux source in most motor type is the alternative electric current in the copper wires which are placed in the stator slots.

Brushless DC Motors (BLDC) are known as high efficiency, long life span, reliable, high power density electric motors(Ali, 2021). They have cool operating temperatures and do not need maintenance over a long time(Abdüssamed, 2020). These features make the BLDC motors most appropriate electric motors for unmanned aerial vehicles(Ahmet Yigit, 2021). The most BLDC motors utilize rare-earth material, neodymium iron boron (NdFeB) magnets to provide enough flux in airgap between stator and rotor. Complicated motor control and high costs because of the magnets are the drawbacks of BLDC motors(Seong-Tae Jo, 2022). Typical BLDC Motor for unmanned aerial vehicles is shown in Figure 1.

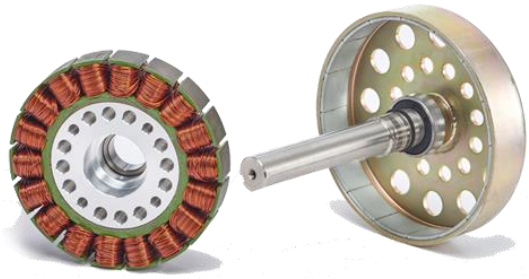

Figure 1. Typical BLDC Motor for unmanned aerial vehicles.

Brushless DC motors can be either interior or outer rotor structure, as shown in Figure 2. The outer rotor structure gives the several following features. First, outer rotor has the larger rotating inertia which helps to reduce/damp the torque ripple and provide smooth stable operation even at low speeds. Second, outer diameter of the outer rotor BLDC is typically higher than internal rotor design. Torque is a function of square degree of outer diameter of the rotor. Hence, for a given motor diameter, an outer rotor motors have higher torque than interior designs. Moreover, bigger airgap area exists in outer design, which enables the higher force to build. Third, bigger outer diameter allows higher pole count which increases the BLDC torque density. Outer rotor structures usually have shorter stack length. In variable loaded applications such as pumps, fans, blowers etc. The high rotor inertia can attenuate the load fluctuations and provide smooth-consant rotor speed. The heat source in the stator is copper power losses. Hence, the stator is exposed to more heat trapping than it is in the interior design. So the current density should be kept lower compared to interior rotor structure as the heat dissipation capability is low inside the motor core part. As can be understood from the literature review, the electric motor study needs multidisciplinary study including electrical, electromagnetics, electronics and mechanics. This paper mainly consists of electrical-electromagnetical design of the unmanned aerial vehicle motor however; other scientific disciplines are not ignored.

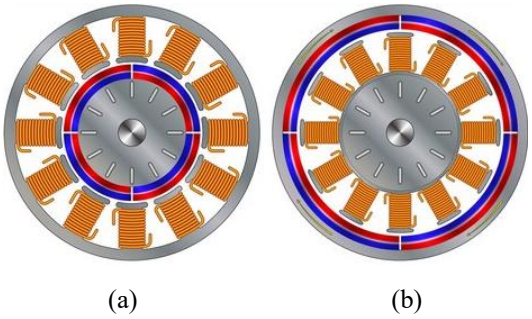

Figure 2. Inner rotor(a) and outer rotor(b) geometries of BLDC motor.

2. Material and Method

2.1. Brushless DC Motor Working Principle

Electric motors are classified as AC and DC electric motors as shown in Figure 3. As contrary to what is known from its name, BLDC motors are alternating current motors in the synchronous motor family. They are widely used in robots, traction control systems, servo drives, fans etc(Berk, 2021).

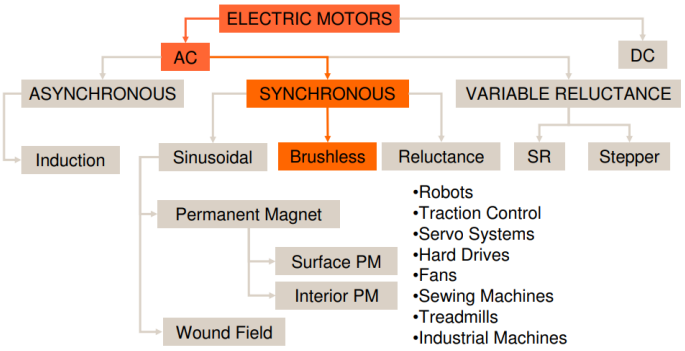

Figure 3. Electric motor type classification (Eduardo, 2008).

Brushless DC motors have trapezoidal back EMF waveform and their excitation method is based on six-step commutation principle(Yusuf, 2015). A typical back EMF and ideal phase excitation waveforms are shown in Figure 4.

Brushless DC motor modeling equations are given in (1-3), where v_{ab} , v_{bc} , v_{ca} are the stator excitation voltages which are provided from BLDC driver, R is the stator one phase resistance and i_a , i_b , i_c are the stator phase currents, L is the phase

inductance. Here, the BLDC motor assumed to have symmetrical phases so the winding resistances and inductances are equal(Ho-Young Lee, 2021).

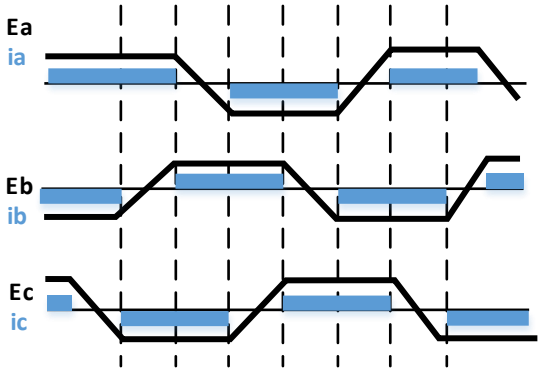

Figure 4. Typical back EMF and phase excitation current waveforms of BLDC motors.

e_a , e_b and e_c back EMF equations are represented in (4-6). Here k_e is the back EMF constant, ω_m is the rotational mechanical speed in radian and $F(\theta_e)$ is the function determined in (7) where changes with rotor position. Generated torque is given in (8) as a function of $F(\theta_e)$, In Y connected BLDC motor the sum of three phase currents should be zero as given in (9). (Stefan, 2005)

$$v_{ab} = R(i_a - i_b) + L\frac{d}{dt}(i_a - i_b) + e_a - e_b \quad (1)$$

$$v_{bc} = R(i_b - i_c) + L\frac{d}{dt}(i_b - i_c) + e_b - e_c \quad (2)$$

$$v_{ca} = R(i_c - i_a) + L\frac{d}{dt}(i_c - i_a) + e_c - e_a \quad (3)$$

$$e_a = \frac{k_e}{2}\omega_m F(\theta_e) \quad (4)$$

$$e_b = \frac{k_e}{2}\omega_m F(\theta_e - \frac{2\pi}{3}) \quad (5)$$

$$e_c = \frac{k_e}{2}\omega_m F(\theta_e - \frac{4\pi}{3}) \quad (6)$$

$$F(\theta_e) = \begin{cases} 1 & 0 < \theta_e < \frac{2\pi}{3} \\ 1 - \frac{6}{\pi}\left(\theta_e - \frac{2\pi}{3}\right) & \frac{2\pi}{3} < \theta_e < \pi \\ -1 & \pi < \theta_e < \frac{5\pi}{3} \\ -1 + \frac{6}{\pi}\left(\theta_e - \frac{5\pi}{3}\right) & \frac{5\pi}{3} < \theta_e < 2\pi \end{cases} \quad (7)$$

$$T_e = k_f\omega_m + J\frac{d\omega_m}{dt} + T_L$$

$$T_e = \frac{k_t}{2}[F(\theta_e)i_a + F\left(\theta_e - \frac{2\pi}{3}\right)i_b + F\left(\theta_e - \frac{4\pi}{3}\right)i_c] \quad (8)$$

$$i_a + i_b + i_c = 0 \quad (9)$$

A typical BLDC motor driving scheme is shown in Figure 5. A 3-phase full bridge inverter with 6 semiconductor switches and their asssociated gate driver circuits are obtained driving signals from microprocessor. Rotor position sensors can be used to increase the motor performance. However, the redundancy is much more important in unmanned aerial vehicles. Hence, signal minimization should be aimed by eliminating the position sensors which can be done by using sensorless motor control algorithm.

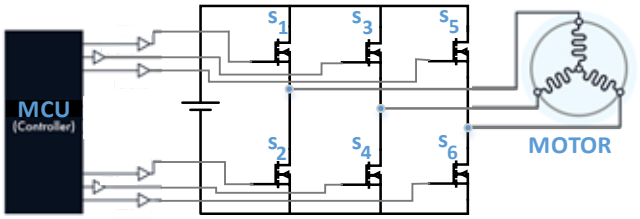

Figure 5. Typical BLDC Motor Control Diagram.

2.2. Brushless DC Motor Design for Unmanned Aerial Vehicles

The design step always starts with design electrical/mechanical limits and performance requirements. First of all, the "Kv" term should be determined as it is highly used in drone applications. "Kv" refers the rotational constant speed of the motor at 1V DC bus voltage. "Kv" unit is the rpm/V. It is measured by revolution of the rotor speed per minute when 1V is applied to the no loaded BLDC motor. Supposing the battery voltage 3S (meaning 3.7Vx3=11.1V) with 500Kv BLDC motor, the unloaded motor speed will be 11.1x500=5550 rpm. By noting that this is an unloaded motor speed, the speed of the BLDC motor will decrease by using propeller in unmanned aerial vehicle. The reason is, as the motor current will increase using propeller, the voltage drop across the winding resistance and cables will increase. Moreover, the permanent magnets will be partially demagnetized temporarily which depends on generated flux linkage by stator magnetic field and magnet temperature (Zhang F, 2019).

Table 1. Motor design input parameters

Kv Rating	**225**	**Kv**
Motor diameter	80	mm
Motor length	21	mm
Rated battery voltage	24	V
Rated battery current	26.1	A
Rated motor power	630	W
Rated speed @max. torque	3500	rpm
Motor mass	205	Gr
Rated torque	1.13	Nm

In this application the input parameters and limits are determined with Table 1. One of the main design criteria is selection of winding type which can be either distributed or concentrated winding. In distributed wounded electric motors, the magnetic field distrbition in the airgap have lower harmonic content which enables higher efficiency and better energy conversion in the airgap (Cemil, 2018).

Table 2. Winding factors of possible slot/pole combinations

STATOR SLOT NUMBER \ ROTOR POLE NUMBER	2	4	6	8	10	12	14	16	18	20	22	24	26	28	30	32	34
3				q < 0.25	q < 0.25		q < 0.25	q < 0.25		q < 0.25	q < 0.25		q < 0.25	q < 0.25		q < 0.25	q < 0.25
6	q > 0.5	0,866		0,866	q < 0.25		q < 0.25	q < 0.25		q < 0.25	q < 0.25		q < 0.25	q < 0.25		q < 0.25	q < 0.25
9	q > 0.5	q > 0.5	0,866			0,866	q < 0.25	q < 0.25		q < 0.25	q < 0.25	q < 0.25	q < 0.25	q < 0.25	q < 0.25	q < 0.25	q < 0.25
12	q > 0.5	q > 0.5		0,866	0,933		0,933	0,866		q < 0.25	q < 0.25		q < 0.25	q < 0.25		q < 0.25	q < 0.25
15	q > 0.5	q > 0.5		q > 0.5	0,866					0,866	q < 0.25		q < 0.25	q < 0.25		q < 0.25	q < 0.25
18	q > 0.5	q > 0.5	q > 0.5	q > 0.5	q > 0.5	0,866	0,902	0,945		0,945	0,902	0,866	q < 0.25	q < 0.25	q < 0.25	q < 0.25	q < 0.25
21	q > 0.5	q > 0.5		q > 0.5	q > 0.5		0,866							0,866		q < 0.25	q < 0.25
24	q > 0.5	q > 0.5		q > 0.5	q > 0.5		q > 0.5	0,866		0,933	0,949		0,949	0,933		0,866	q < 0.25
27	q > 0.5	q > 0.5	q > 0.5	q > 0.5	q > 0.5	q > 0.5	q > 0.5	q > 0.5	0,866			0,945			0,945		
30	q > 0.5	q > 0.5		q > 0.5	q > 0.5		q > 0.5	q > 0.5		0,866	0,874		0,936	0,951		0,951	0,936
33	q > 0.5	q > 0.5		q > 0.5	q > 0.5		q > 0.5	q > 0.5		q > 0.5	0,866						
36	q > 0.5	q > 0.5	q > 0.5	q > 0.5	q > 0.5	q > 0.5	q > 0.5	q > 0.5		q > 0.5	q > 0.5	0,866	0,867	0,902	0,933	0,945	0,953
39	q > 0.5	q > 0.5		q > 0.5	q > 0.5		q > 0.5	q > 0.5		q > 0.5	q > 0.5		0,866				
42	q > 0.5	q > 0.5		q > 0.5	q > 0.5		q > 0.5	q > 0.5		q > 0.5	q > 0.5		q > 0.5	0,866		0,89	0,913
45	q > 0.5	q > 0.5	q > 0.5	q > 0.5	q > 0.5	q > 0.5	q > 0.5	q > 0.5		q > 0.5	q > 0.5	q > 0.5	q > 0.5	q > 0.5	0,866		
48	q > 0.5	q > 0.5		q > 0.5	q > 0.5		q > 0.5	q > 0.5		q > 0.5	q > 0.5		q > 0.5	q > 0.5		0,866	0,857

Unbalanced Winding

Non-symmetrical Winding

However, distributed wounded electric motors have higher end-turn length and usually have bigger winding resistance which cuts the efficiency and make the motor operating temperature higher, as well. Moreover, its manufacturing process is difficult. However, concentrated windings can be quickly and cheaply wound by winding machine. Other advantages are short end-turns, less winding resistance. These features make the concentreated winding method suitable for unmanned aerial vehicles (UAVs), as more compact motor design is possible with this method. A major challenging issue in the concentrated winding motor is selection of suitable slot/pole number of BLDC. Otherwise, its performance would be poorer than distributed wound BLDC motor.

Table 2 shows the winding factors of possible slot/pole combinations. It should be noted here that green highlights have highest winding factor, however yellow highlights are worse winding factor than green. This table can be extended to very high pole/slot count. However, as the motor outer diameter is limited by 80mm, very high numbers would not be realistic as the manufacturing difficulty will be much more. Winding factor is one of the important performance parameter which highly depends on pole/slot combination and can maximize the back EMF voltage with proper selection as represented in (10). Here, p is the pole pair number, ω_m is the mechanical angular speed, N is the total number of serial turns per phase, k_w is the winding factor and k_{st} is the stacking factor. From Table 2, 24 slot number and 28 pole is selected to reach highest motor power density. Hereafter, as the geometrical limits are already determined by the application, parametric optimization is performed for each design parameter which are teeth geometry, airgap length, magnet grade and its geometry, wire diameter and number of turns, number of parallel path etc. we will not go into detail as the parametric optimization tools are already well known by FEA software packages. Instead, the final optimized geometry FEA analyses results and its effects on the motor performance were deeply studied.

$$\hat{E} = p\omega_m N \emptyset_g k_w k_{st} \qquad (V_{peak}) \tag{10}$$

Figure 6 shows the magnetic field density (B) of developed outer rotor BLDC at no load condition, the BLDC model is established in Ansys-Electronics. Silicon based lamination material is used in stator stack. Silicon steel lamination material saturates around 1.65-1.7 Tesla. In the figure, the result shows that stator teeth reach to 1.75 Tesla magnetic field density. As a result, some part of the stator is facing saturation which increases the iron losses consisting hysteresis and eddy current losses represented in (11-12). Here K_h and K_e are hysteresis and eddy current loss coefficient depending on material properties, B_{max} is the maximum magnetic field density in the designated volume, n is the factor and its value is commonly taken 1.5-2 in electric machine applications. f is the electrical frequency and t is the lamination thickness. It is clear that magnetic field density strongly increases the total iron loss. As a trade off, trying to keep magnetic field density low will result in the motor getting bigger and heavier.

$$P_{hysteresis} = K_h {B_{max}}^n f \qquad (W/m^3) \tag{11}$$

$$P_{eddy} = K_e {B_{max}}^2 f^2 t^2 \qquad (W/m^3) \tag{12}$$

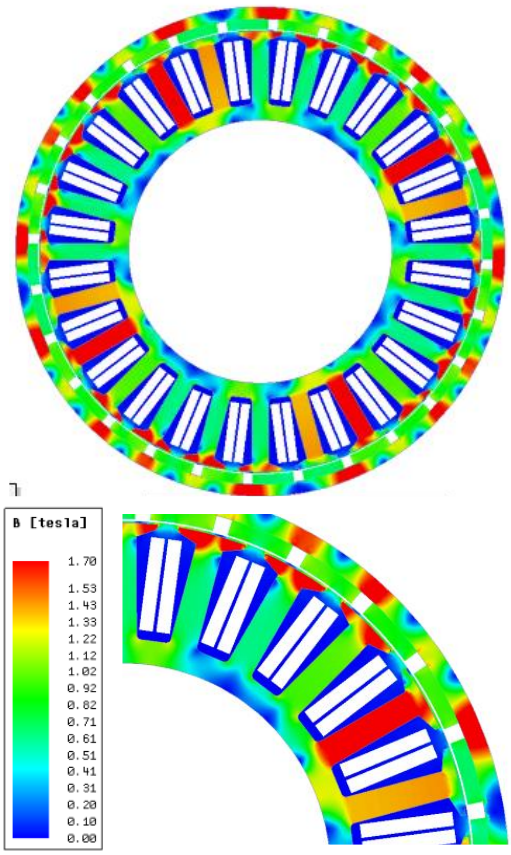

Figure 6. Magnetic field density of developed outer rotor BLDC at no load.

The resultant back EMF waveforms are given in Figure 7. The results show that phase induced voltages are similar to trapezoidal waveshape and relatively lower harmonic content than line-to-line back EMFs. However, this is known that phase voltages play an important role in torque ripple. The motor is designed to be excited in a six-step pulse, so the back EMF waveforms are suitable for this excitation type. The other performance metric is the cogging torque. In fan applications the cogging usually can be ignored, however, this is known that cogging torque will cause acoustic noise and shortens the life of the bearings as it causes vibration in light load(Jacek F. Gieras, 2003). Hence, it should be minimized in unmanned aerial vehicles as the noise is critical issue in missle applications(Kun Xia, 2017).

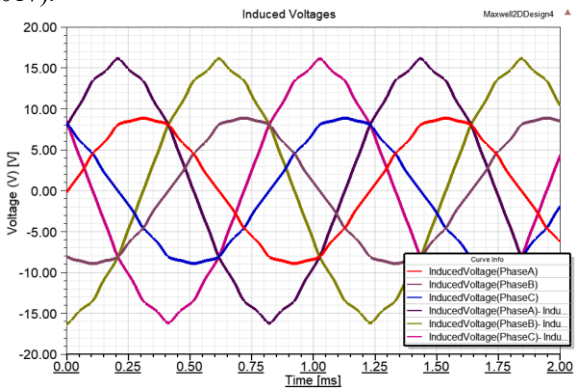

Figure 7. The Back EMF waveforms of developed BLDC motor.

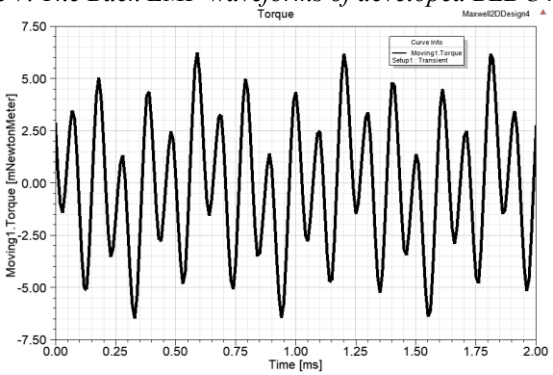

Figure 8. The cogging torque waveform of the developed BLDC.

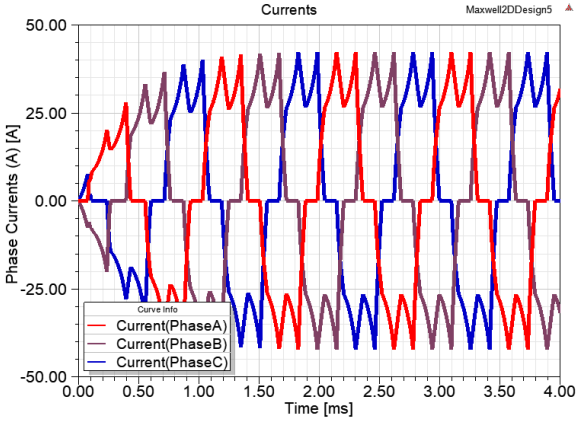

(a)

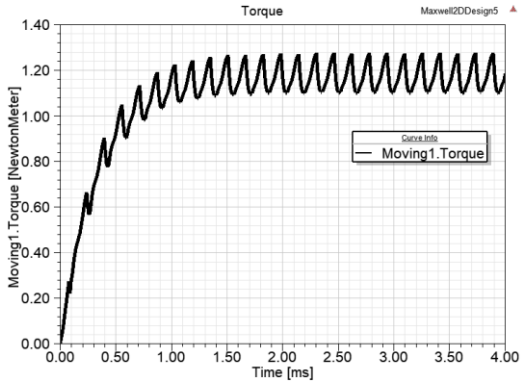

(b)

Figure 9. Phase currents(a) and generated electromagnetic torque(b) of developed BLDC motor.

2.3. Experimental Study

The developed outer rotor BLDC was manufactured to verify the design stage. First of all, mechanical design is executed as shown in Figure 10. As it is unmanned aerial vehicle application, minimum motor mass is one of the biggest goals. Hence, aluminium 7075 aviation material is used in the motor frame. Aluminium 7075 series has very high yield strength feature compared to conventional 6063 or 5000 series aluminium.

Winding is the challenging step in the production process. Maximal copper usage is always aimed to reach high performance and high efficiency in the BLDC motor. However, as it is outer rotor structure, slot fill factor is relatively worse than inner rotor structure. The final produces BLDC motor picture is shown in Figure 11.

Figure 10. Mechanical design of outer rotor BLDC motor.

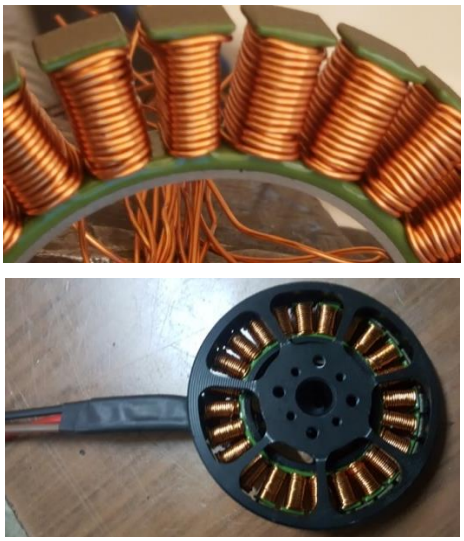

Figure 11. Winding stage and final picture of produced BLDC motor.

The produced BLDC motor is tested in the dynamometer which includes dynamic torque sensor and electromagnetic powder brake as a passive load. Typical six-step excitation voltage in the test progress is given in Figure 13. The test procedure is performed in a wide speed and torque range to obtain the motor and driver efficiency. The measured efficiency map of the developed BLDC motor is drawn with propeller load characteristic curve. The result shows that, developed BLDC motor efficiency is maximized in the wide speed operating range which enables to reach highest system efficiency in the unmanned aerial vehicle applications.

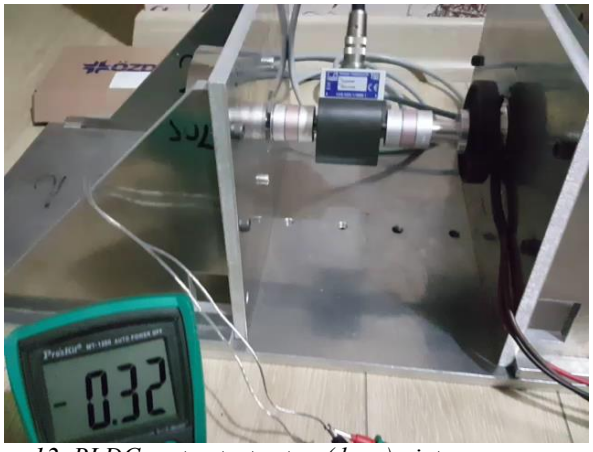

Figure 12. BLDC motor test setup (dyno) picture.

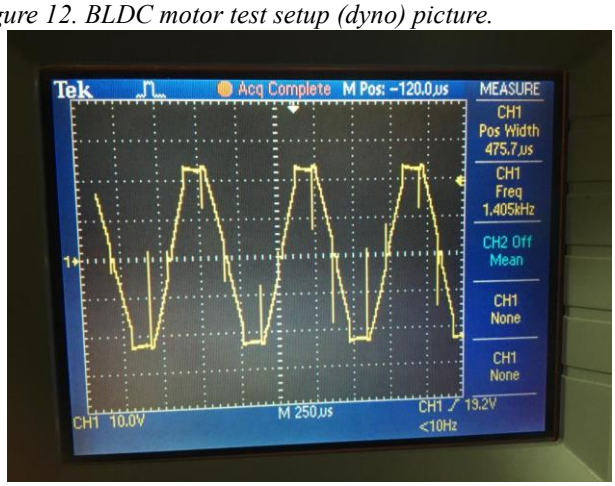

Figure 13. Measured one phase six-step excitation voltage waveform.

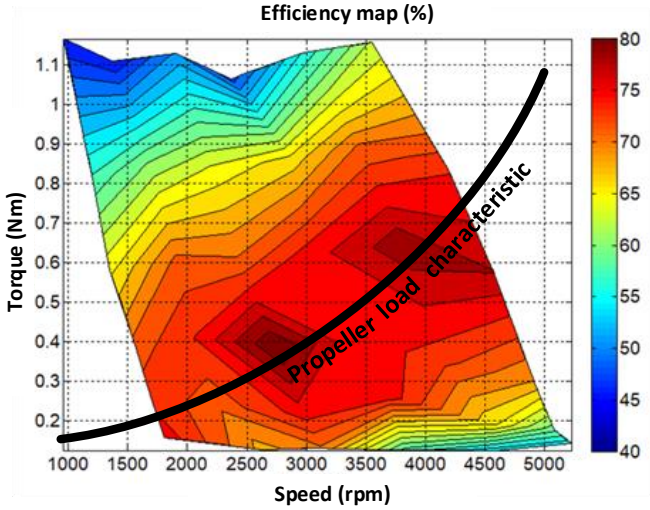

Figure 14. the efficiency map of developed BLDC motor and the propeller load characteristic.

3. Conclusion

In this study, 650W, 3500rpm with 225Kv, 5kg traction force BLDC motor is developed by using multidisciplinary study. Unmanned aerial vehicle total system efficiency is highly depends on traction motor energy conversion efficiency as the most of the stored energy in the battery is used by motors. Hence, BLDC motor efficiency should be maximized and optimized not just in a motor side. In addition, BLDC motor and propeller load characteristic curve should be taken into account together. The results show that the harmoniousness of BLDC motor and the propeller enables to reach high system efficiency. The simulation and experimental results clearly show that this goal is achieved in a wide speed range. The similar method is planned to be executed for high power BLDC motors in UAV application.

4. Acknowledge

Financial support for this research was provided by YASA Motor Technologies, Bursa Turkey.

References

Mithra SivaKumar, & Naga Malleswari TYJ (2021). A literature survey of unmanned aerial vehicle usage for civil applications. *Journal of Aerospace Technology and Management,* 13, 1-8. https://doi.org/10.1590/jatm.v13.1233

Taha Benarbia, & Kyandoghere Kyamakya (2022). A Literature Review of Drone-Based Package Delivery Logistics Systems and Their Implementation Feasibility. Sustainability, 14 (360), 1-15. https://doi.org/10.3390/su14010360

Emanuele Adorni, & Anastasiia Rozhok, Roberto Revetria, Mikhail Ivanov (2021). Literature Review on Drones Used in the Surveillance Field. *Proceedings of the International Multi Conference of Engineers and Computer Scientists,* 1-6.

Seong-Tae Jo, & Hyo-Seob Shin, & Young-Geun Lee, & Ji-Hun Lee and Jang-Young Choi (2022). Optimal Design of a BLDC Motor Considering Three-Dimensional Structures Using the Response Surface Methodology. *MDPI Energies*, 15, 1-13, https://doi.org/10.3390/en15020461

Eduardo Viramontes (2008). Hands-on Workshop: Motor Control Part 4 - Brushless DC Motors Made Easy. *FreeScale Technology Forum.*

Kaynak, Berk. & Arabul, A. Y., "Sizing, Design and Analysis of Fixed Wing Unmanned Aerial Vehicle's Wing", 6th International Mardin Artuklu Scientific Researches Conference, Mardin, Türkiye, 25 - 27 Haziran 2021, ss.74-81.

Yusuf Yasa,& Erkan Mese (2015). Thermal Assessment of Outer Rotor Direct Drive Gearless Small-Scale Wind Turbines, World Academy of Science, Engineering and Technology International Journal of Environmental and Ecological Engineering, v9-8, 1004-1008.

Ho-Young Lee,& Seung-Young Yoon,& Soon-O Kwon, & Jin-Yeong Shin, & Soo-Hwan Park and Myung-Seop Lim (2021). *A Study on a Slotless Brushless DC Motor with Toroidal Winding. Processes*, 9, 1-19, *https://doi.org/10.3390/pr9111881.*

Stefan Baldursson (2005). BLDC Motor Modelling and Control – A Matlab®/Simulink® Implementation. *Master Thesis, Chalmers Tekniska Högskola.*

Jacek F Gieras (2003). Analytical approach to cogging torque calculation in PM brushless motors, IEEE International Electric Machines and Drives Conference – IEMDC, https://doi.org/10.1109/IEMDC.2003.1210329.

Kun Xia, Zhengrong Li, Jing Lu, Bin Dong, and Chao Bi (2017). Acoustic Noise of Brushless DC Motors Induced by Electromagnetic Torque *Ripple. Journal of Power Electronics, 17 (4), 963-971.* https://doi.org/10.6113/JPE.2017.17.4.963.

Ali Bahadır, Ömer Aydoğdu (2021), DSP Tabanlı Fırçasız Doğru Akım Motorunun Bulanık Mantık ile Kontrolü. European Journal of Science and Technology No. 23, pp. 427-434, April 2021. https://doi.org/10.31590/ejosat.877627

Abdüssamed Tabak (2020), Fırçasız Doğru Akım Motorlarının Hız Kontrolünü Gerçekleştirmek İçin PID/PD Kontrolcü Tasarımı ve Performans İncelemesi. European Journal of Science and Technology No. 19, pp. 145-155, August 2020. https://doi.org/ 10.31590/ejosat.707004

Arabul, Ahmet. Yigit, Kurt, E., Keskin Arabul, F., Senol, İ., Schrötter, M., Bréda, R., & Megyesi, D. (2021). Perspectives and Development of Electrical Systems in More Electric Aircraft. International Journal of Aerospace Engineering, 2021.

Zhang, F., Yu, S., Wang, Y., Jin, S., Jovanovic, M.G (2019), Design and performance comparisons of brushless doubly fed generators with different rotor structures. IEEE Transactions on Industrial Electronics, 2019: 66(1), 631-640. https://doi.org/0.1109/TIE.2018.2811379.

Cemil Ocak (2018), Design and performance comparison of four-pole brushless DC motors with different pole/slot combinations, The International Journal of Energy & Engineering Sciences, 2018, 3(3), 69-78.